machines

MDPI

Article

Design of a Digital Twin for an Industrial Vacuum Process: A Predictive Maintenance Approach

Mohammad F. Yakhni [1,2,3], Houssem Hosni [1,2,4], Sebastien Cauet [1,*], Anas Sakout [2], Erik Etien [1], Laurent Rambault [1], Hassan Assoum [3] and Mohamed El-Gohary [3,5]

1 Laboratoire d'Informatique et d'Automatique pour les Systemes, Université de Poitiers, 86000 Poitiers, France
2 Laboratoire des Sciences de l'Ingénieur pour l'Environnement, CNRS, Université de La Rochelle, 17000 La Rochelle, France
3 Mechanical Department, Beirut Arab University, Campus Debbieh, P.O. Box 11-50-20, Riad El Solh 11072809, Lebanon
4 Societé Girardeau, 86110 Mirebeau, France
5 Mechanical Department, Alexandria University, Al Azaritah WA Ash Shatebi-Qesm Bab Sharqi, Alexandria Governorate 5424010, Egypt
* Correspondence: sebastien.cauet@univ-poitiers.fr

Abstract: The concept of a digital twin is increasingly appearing in industrial applications, including the field of predictive maintenance. A digital twin is a virtual representation of a physical system containing all data available on site. This paper presents condition monitoring of ventilation systems through the digital twin approach. A literature review regarding the most popular system faults is covered. The motor current signature analysis is used in this research to detect system faults. The physical system is further described. Then, based on the free body diagram concept and Newton's second law, the equations of motion are obtained. Matlab/Simulink software is used to build the digital twin. The Concordia method and the Fast Fourier Transform analysis are used to process the current signal, and physical and numerical system current measurements are obtained and compared. In the final step of the modeling, specific frequencies were adjusted in the twin to achieve the best simulation. In addition, a statistical approach is used to create a complete diagnostic protocol.

Keywords: condition monitoring; motor current signature analysis; fan/motor system; digital twin; dynamic modeling; statistical approach

Citation: Yakhni, M.F.; Hosni, H.; Cauet, S.; Sakout, A.; Etien, E.; Rambault, L.; Assoum, H.; El-Gohary, M. Design of a Digital Twin for an Industrial Vacuum Process: A Predictive Maintenance Approach. *Machines* **2022**, *10*, 686. https://doi.org/10.3390/machines10080686

Academic Editor: Ahmed Abu-Siada

Received: 12 July 2022
Accepted: 10 August 2022
Published: 12 August 2022

1. Introduction

In industrial installations, ventilation systems are numerous and increasingly require continuous monitoring. Any sudden failure of these components can result in significant damage. Condition Monitoring (CM) is a growing technology that enables the identification of incipient defects. It can prevent unexpected failure of critical elements, increasing the life of components while decreasing maintenance downtime and costs. These systems mainly consist of an electric motor, a fan, ducts, bearings, transmission shafts, etc. [1]. In most cases, the fan is not connected directly to the motor, mainly to achieve two objectives. The first one is to protect the motor, since the fan is exposed to environmental disturbances and withstands different operating conditions, while the second goal is to control the rotation speed and torque of the fan by adjusting the diameter of gears or pulleys [2]. In summary, it can be said that this type of system can be divided into two main parts. The first is the electric motor, which we will consider in this article as an Induction Motor (IM) since it is the most commonly used in industrial sectors, including ventilation and suction systems [3]. The second part is the purely mechanical system that includes the rest of the components. So, in this article, we will deal with these systems as fan/motor systems.

The IM is subjected to several defects, and the majority of them can be classified as shown in Table 1, where each malfunction and its type are listed, along with the work

environment of each motor. As for the fan part, it can be affected by various faults, like any rotating system, but the most significant are: fan imbalance [4], shafts misalignment [3], belt defects [5], and last but not least, bearing faults [6].

Table 1. Common IM defects and work environments.

Fault	Fault Type	Motors Phases	Motors Power (KW)	References
Stator faults	Electrical	Three-phases	1.48; 2.2	[7,8]
Unbalanced voltage	Electrical	Three-phases	0.75; 4	[9,10]
Broken rotor bar	Mechanical	Three-phases	1.1; 7.5	[11,12]
Eccentricity	Mechanical	Three-phases	1.1; 2.2	[13,14]
Bent shaft	Mechanical	Three-phases	0.8; 0.373	[15,16]
Bearing	Mechanical	Three-phases	3; 0.425	[17,18]

These faults need to be predicted at an early stage, and appropriate actions must be taken to ensure the smooth running of the system. There are several methods to achieve this goal, but vibration analysis is the most popular method for condition monitoring. Acoustic monitoring is a viable option because vibrations create acoustic noise. However, as these methods are expensive due to the additional transducers required, they are only appropriate for large machinery or highly critical applications such as wind turbines [19], milling and grinding processes [20]. All system malfunctions affect the IM, either directly or indirectly, so Motor Current Signature Analysis (MCSA) can be employed for CM. This method is part of the general topic called Electrical Analysis, which has proven to be a very efficient and practical approach since the current and voltage signals are easy to monitor. This type of signal reduces the number of transducers installed since current and voltage transducers are already installed for control, safety, energy, and other reasons. Electrical signals have been used to detect and locate not only electrical faults but also mechanical faults in the system components [21]. MCSA has undergone significant development in the last 30 years [22]. Numerous studies and works have been reported, such as the book by Saad et al. [23] and the one by Thomson [24], that discuss CM using electrical signature analysis. All these advantages and the effectiveness of the MCSA prompted us to adopt this approach in this research. Based on the above, and the fact that this article takes into account the evolution of industrial sectors—in particular today's fourth industrial revolution (industry 4.0), which does not require human beings—production can be done with cyber-physical links with much less error and high reliability. With this revolution, products are becoming capable of sensing their own condition and that of their environment, coupled with the ability to process and communicate this data, enabling the development of digital twins that can simulate physical system operation, track energy consumption (monitoring electrical signatures), detect system faults (electrical, mechanical, vibratory), and allow experimentation that is hard to carry out with actual installations [25].

Since the concept was first coined by John Vickers and Michael Grieves [26], many authors have attempted to define the term digital twin, beginning with the aerospace industry [27], focusing on the structural mechanics, materials science, and long-term performance prediction of air- and spacecraft [28]. With the growth of Industry 4.0, the focus has shifted to manufacturing and smart products [27]. In this context, the digital twin can contribute to information continuity throughout the product life cycle [29,30], the virtual commissioning of (manufacturing) systems [31], and decision support and predictions of system behavior in the product development phase and in all subsequent phases of the life cycle on the basis of computer-aided implementations [32]. The digital twin as a concept contains three major parts, which are the physical objects in the real space, the virtual objects in the virtual space, and the data and information connections that link the virtual and real products [33]. The concept of the numerical model has been adopted in many previous kinds of research, and it has given satisfactory results in achieving its objectives; for example, to study the dynamics of a belt-pulley-shaft system, a numerical model was developed by [34]. The investigation of the accelerating transient vibrations of

a rotor system was done by [35]. The numerical model was utilized by [36] to monitor an aero-engine dual-rotor system with a fan blade out. The digital twin has many uses, even simulating the operation of cars on the road [37] or CNC machine tool [38], etc.

The uses of the digital twin have been mentioned generally in the above. Now we will switch to what is related to the topic of this research and discuss some of the previous research that has used this approach in the area of fault diagnosis. The concept was used by [39] to monitor an electric submersible pump towards a mechanical seal failure, and they obtained good results. The paper published by [40] proposes an intelligent fault diagnosis method for a triplex pump based on digital twin and deep transfer learning. The proposed method has been experimentally validated and gives satisfactory results. Another study [41], was inspired by the fact that transfer diagnosis scenarios are limited to the experimental domain, the inter-domain marginal distribution and conditional distribution are difficult to simultaneously align, and each source–domain sample is assigned equal importance during the domain adaptation process; thus, the study proposed a new joint transfer network for unsupervised bearing fault diagnosis from the simulation domain to the operational field. The digital twin approach was used by [42] in the intelligent manufacturing area to monitor the health of a rotating machine. The main challenge of this study was the nonlinear dynamics and uncertainty involved in the machine degradation process. It successfully overcame this challenge and achieved the desired goal, as evidenced by the results.

After reviewing some of applications of the digital twin, we move on to the content of this paper, where we use this concept for the condition monitoring of a ventilation system. The most common types of faults have been examined and considered in the proposed approach, in order to create an alarm that can warn maintenance managers in the industry of the severity of each malfunction, based on a statistical study of a specific type of fault, and apply it to the other defects; thus, there is now a reference that takes into account the state that the physical system should be in, whether looking at fault signatures or power consumption. In general, we created a software version of the actual system that allows users to experience what they cannot do in reality. Experimental and simulations results prove the effectiveness of this developed technique. The use of this approach has been limited in this article to a specific type of industrial system (ventilation systems), but with some modifications, it can be used with a different framework.

This article is organized into four main sections. Section 2 describes the physical system, and then deals with the development of the digital twin. The conditional maintenance technique used in this research is also outlined. After that, the re-sampled signal is exploited by a statistical diagnostic procedure. The obtained experimental and simulation results are presented in Section 3 and discussed. The last section is the conclusion of this paper, with a discussion of possible future work.

2. Materials and Methods

2.1. Description of the Physical System

The Municipal Technical Center (MTC) of Poitiers, France, is a state-owned structure that participates in the implementation of projects for the city via different means. It is divided into several departments and contains several workshops. Among its workshops, the most prominent is carpentry. The current installation in the MTC has 11 machines, 4 of which work simultaneously (panel saw, combi-sander, planer, and long belt sander). The 3D visual of the wood dust-extraction system is shown in Figure 1.

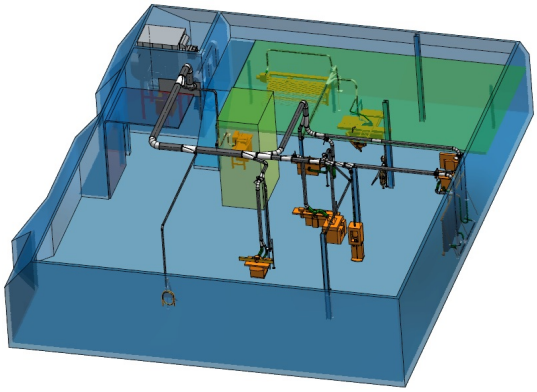

Figure 1. The 3D visual of the wood dust-extraction installation at the MTC.

In this application, we are mainly interested in the control of the operating state of the fan/motor part. The system to be monitored is shown in Figure 2. It is composed of an asynchronous IM, where its characteristics are presented in Table 2, and the mechanical system including all other components. Figure 3 provides a detailed illustration of this system, while the labels for each component are listed in Appendix A, at the end of the paper.

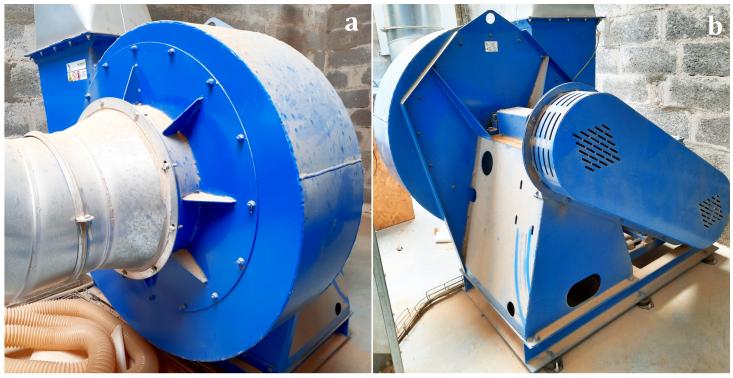

Figure 2. The fan/motor system (**a**) fan side (**b**) transmission side.

Table 2. The motor characteristics.

Supply	Voltage (V)	Frequency (Hz)	Current (A)	Power (KW)	Cos (ϕ)	Speed (rpm)
Three-Phase	400 Delta	50	51.6	30	0.9	2950

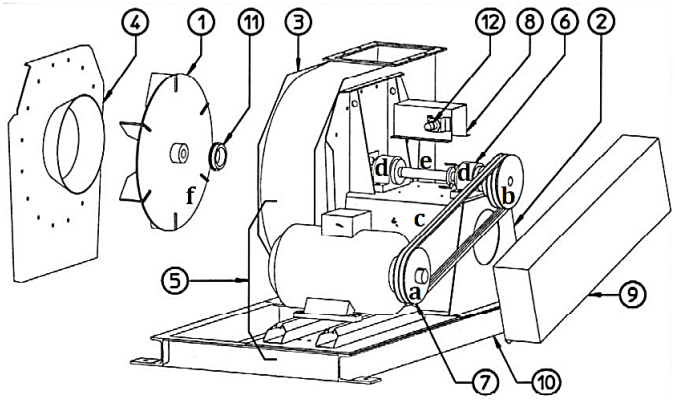

Figure 3. The physical system with label.

We had previously indicated that the system being dealt with is divided into two parts, the electric motor (IM) and the mechanical part (the fan and the transmission system). This system mainly consists of Pulley 1 (marked "a") connected directly to the motor. The power is transmitted from the motor to Pulley 2 (marked "b") by three belts (marked "c"), where each belt has a length (L) equal to 2300 mm type SPB Vbelt. The fan (marked "f") is connected to Pulley 2 by a transmission shaft (marked "e"), and has a diameter of 45 mm and length of 80 mm. The diameter of Pulleys 1 (R_{p1}) and 2 (R_{p2}) are 160 and 225 mm, respectively. The two bearings (marked "d") that support this shaft are type 22210 EK. The fan has eight blades that are made of steel 60A, like the rest components. Other parts (labeled from "1" to "12") have little effect on the basic function of the system, so we ignored their influence during the modeling process. The label of each part is given in Appendix A at the end of the paper.

After identifying the system concerned and its components, we now move on to the modeling stage, which takes place in the following section.

2.2. Developing of the Digital Twin

2.2.1. Mathematical Model

The mechanical part of the ventilation (suction) system is composed of three basic masses, which are pulley 1, pulley 2, and the fan, so it is considered to have three degrees of freedom. Using Newton's second law of motion and the concept of the free-body diagram, Figure 4 can be drawn, and the motion equations have been obtained and presented in Equations (1)–(3) for each mass:

- Pulley 1:

$$J_1\ddot{\theta_1} = T_e - 2K_b(R_{p1}\theta_1 - R_{p2}\theta_2) \quad (1)$$

- Pulley 2:

$$J_2\ddot{\theta_2} = 2K_b(R_{p1}\theta_1 - R_{p2}\theta_2) - K_s(\theta_2 - \theta_F) - B_r(\dot{\theta_2} - \dot{\theta_F}) \quad (2)$$

- The fan:

$$J_F\ddot{\theta_F} = K_s(\theta_2 - \theta_F) + B_r(\dot{\theta_2} - \dot{\theta_F}) + T_a \quad (3)$$

where θ_1, θ_2, and θ_F are the rotation angle of pulley 1, pulley 2, and the fan respectively, while J_1, J_2 and J_F are the polar moments of inertia of the three masses, respectively, as the rotation angle. T_e is the electromagnetic torque resulting from the motor and T_a is the load torque, described in the next section. The three belts have been modeled as flexible components with equivalent linear stiffness K_b, and the shaft has a torsional stiffness K_s. The two bearings have an overall friction coefficient of B_r.

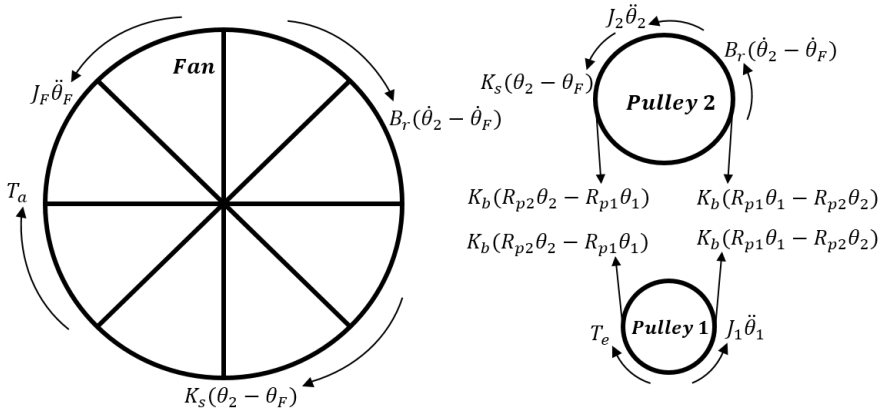

Figure 4. Free-body diagram of the fan/motor system.

2.2.2. System Defects

This system is subject to several defects, which have been combined in the model as torques and their value has been added to T_a, so that the value of Ta has evolved as shown in Equation (4).

$$T_a = (Q \times \Delta P / w) + T_d \quad (4)$$

Where Q, ΔP, and w are the flow rate, pressure difference, and the rotation speed of the fan, while T_d is the torque resulting from the presence of a defect in the system, that has been implanted as a sinusoidal, shown in Equation (5), and varies with time (t), has amplitude A, and frequency f_d:

$$T_d = A \times cos(2\pi f_d t) \quad (5)$$

In this article, we deal with the most popular system faults, where each one has a particular frequency proportional to the rotation speed. Table 3 presents these defects with their frequencies in the torque reference. Note that f_r is the rotational frequency of the rotor, f_e is the fundamental frequency of the power supply, n_b = 10 is the number of balls in each bearing, N_n = 28 is the number of notches in the stator, N_b is the number of fan blades, and p = 1 is the pole pairs number.

Table 3. Types and defects frequencies.

Defect	Frequency (Hz)	Reference
Bearing inner ring	$0.6 \times n_b \times f_r$	[43]
Ball bearings	$0.4 \times n_b \times f_r$	[43]
Belts	$2\pi \times R_{p1} \times f_r / L$	[44]
Broken rotor	$2 \times (f_e - f_r)$	[45]
Notch harmonics	$N_n \times f_r / p$	[46]
Eccentricity	f_r	[47]
Fan imbalance	$N_b \times f_r$	[47]
Misalignment	$2 \times f_r$	[39]

Since we are dealing with a system functioning in the industry, the possibility of creating defects is actually not possible, so we will use simulation to achieve this goal. Equation (5) indicates that the frequency of the defect changes according to its type as shown in Table 3. As for the severity of this defect, it is related to the variable, A. Therefore, in order to change the severity of the defects we will create, we will use a random variable that will represent the value of A, where we will set its mean value and the degree of change about it.

2.2.3. Modeling

After obtaining the necessary mathematical equations, it became possible to model the ventilation system, or more precisely, the fan/motor system in our case. The Matlab/Simulink software R2021b was used to perform this task. Let us start with the three equations of motion, Equations (1)–(3), and build their Simulink model shown in Figure 5, while Figure 6 shows the overall diagram. The mechanical torque is the sum of all moments on the fan that has a value equal to $J_F \ddot{\theta}_F$. This torque is used as feedback to the induction motor as the load torque in a realistic situation. The IM is powered by a three-phase AC source, and some noise has been added to the stator current, to make it closer to reality.

Once the modeling is done, a pilot digital twin model of the fan/motor system is constructed as shown in Figure 7.

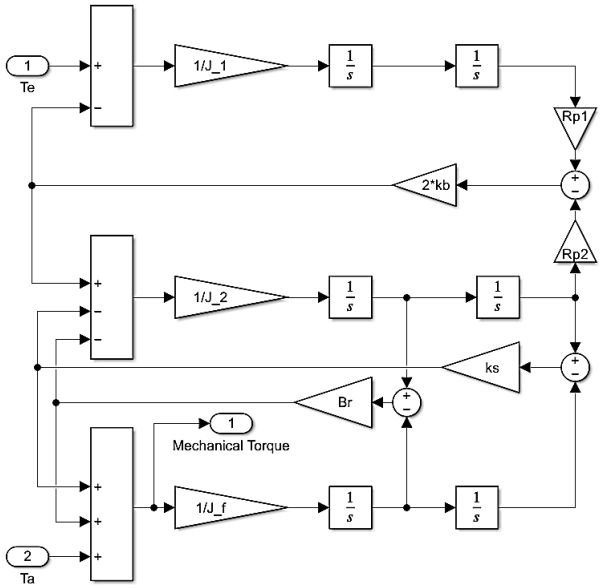

Figure 5. Similink model of the three equations of motions.

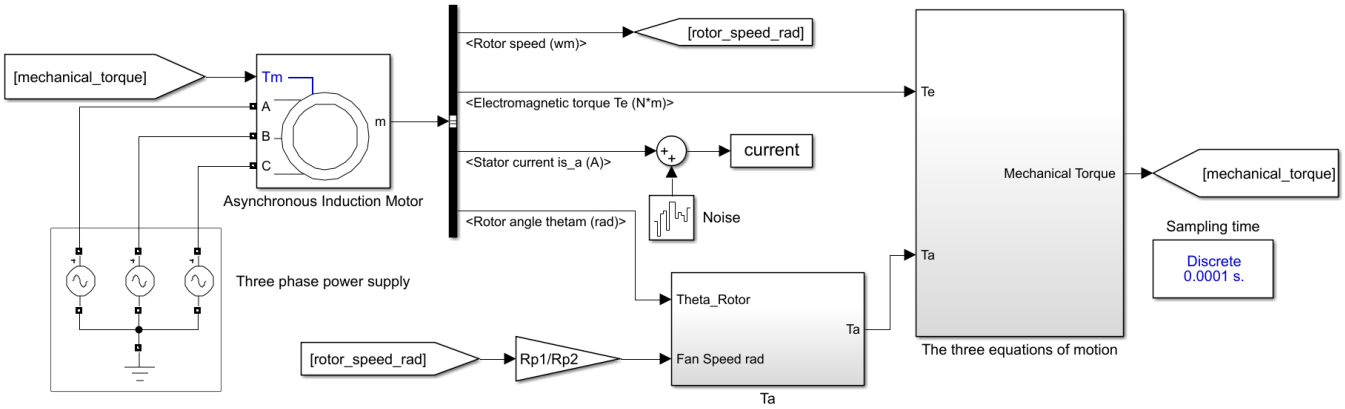

Figure 6. The overall Simulink model.

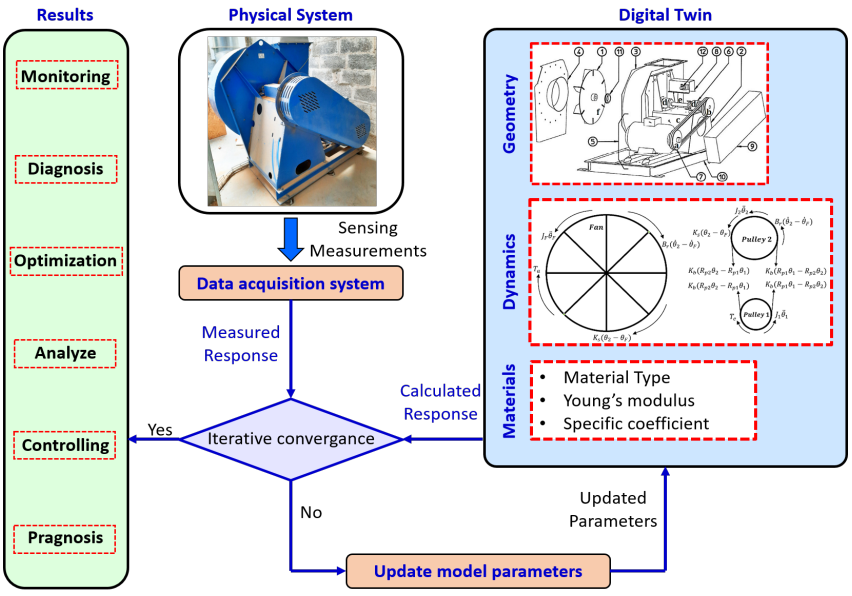

Figure 7. Illustration of the developed digital twin model of the fan/motor system.

Figure 7 shows, under the title "Digital Twin" in the blue part, the stages of building the digital twin, which begins with understanding and studying the physical system, its components and geometries, and then moving to the modeling stage by creating the free body diagram, then the use of the Newton's second law of motion to obtain the system equations. The digital twin provides condition monitoring administration in light of Simulink models created by real systems and information acquired in the real world. To develop a computerized model to accurately and continuously monitor the state of the real framework, it is important to examine a methodology for constant updating between the computerized model and the real system. The current system collects information in a bottom-up manner. It first acquires different information about the subsystem boundaries and then collects information about the perception at the frame level. Finally, it combines this information from the subsystems to the framework as a mark of the well-being of the entire framework. This granular perspective works with the resulting foundation of the Digital Twin model in light of the actual components. In addition, the physical world needs to transfer many kinds of information to the digital environment, such as operating conditions, working situations, sensor records, and more. The physical system needs standard data communication schemes to accomplish a uniform conversion of the various communication protocols or interfaces and a standard packaging of the information. Through these data communication features, the multi-type and multi-scale information is standardized, cleaned and packaged by the physical system, and then loaded to the Digital Twin model in the virtual world. This significantly improves the performance of the twin.

In our case, we only used current and voltage sensors, since we use MCSA technology. These sensors provide us with the real voltage and current signals. By analyzing any of these signals using the methods that will be explained later, we notice that they contain certain frequencies, and each one belongs to a specific part of the system. These frequencies are our target, we monitor them and update the signal received from the digital twin to contain the same frequencies and values, so as to obtain an iterative convergence between the measured and the calculated response, as illustrated in Figure 7, and demonstrated in the results achieved in this study.

Let us move on to the next step: the CM. As mentioned in the introduction, the technique that will be used in this article to perform this task is the MCSA. The following section will address this point.

2.3. Electrical Analysis

2.3.1. Motor Current Signature Analysis (MCSA)

The MCSA method is generally considered to be a popular fault diagnosis technique for identifying the common malfunction of electric rotating equipment. This method is part of the general topic known as electrical analysis. Defects happening in the components of the system can cause fluctuations in torque and eccentricity due to the current and voltage variations [48,49]. These fluctuations cause phase modulations (PM) of the current in the event of torque variation, and amplitude modulations (AM) in the case of dynamic eccentricity variations [50]. The general form of the stator current can be given as shown in Equation (6):

$$I(t) = A(t)cos(\theta(t)) \tag{6}$$

where $A(t)$ and $\theta(t)$ represent, respectively, the instantaneous amplitude and the instantaneous phase. In the case of sinusoidal perturbations, the expressions of the modulated current are given as Equations (7) and (8):

$$A(t) = I.[1 + \alpha cos(2\pi f_{AM} t + \Phi_{AM})] \tag{7}$$

$$\theta(t) = 2\pi f_e t + \beta cos(2\pi f_{PM} t + \Phi_{PM}) + \Phi_I \tag{8}$$

where α, f_{AM}, and Φ_{AM} represent, respectively, the modulation index, the frequency of the modulating signal, and the initial phase for AM modulation, as well as β, f_{PM}, and Φ_I for PM modulation.

The separation of the fault elements in the currents is much more difficult than in vibration measurement as the signal-to-noise ratio is much lower and the fundamental electrical element has a large amplitude and masks the desired frequencies. One way is to suppress this fundamental in order to amplify the defect frequencies [51]. The simplest solution, however, is to demodulate currents in amplitude or in phase. Since a long time ago, numerous demodulation techniques have been suggested. They can generally be categorized based on two factors: mono or multi-dimensional approaches, and online or offline methods. Table 4 lists the methods respecting this classification.

Table 4. Current demodulation techniques.

Method	Dimension	Type	Reference
Recursive identification	Mono-dimensional	Online	[52]
Teager–Kaiser Energy	Mono-dimensional	Online	[53]
Concordia Transform	Multi-dimensional	Online	[54]
Hilbert transform	Mono-dimensional	Offline	[55]
Principal Component Analysis	Multi-dimensional	Offline	[56]

In this article we choose to use the Concordia transform, because the three phase currents are available and this method can be achieve the online detection of system faults. The following section provides a brief description about this method.

2.3.2. Concordia Transform

When the three currents are available, the simplest approach to highlight the AM and PM modulations is to combine them by applying the Concordia transform. This group of methods is known as the Park Vector Approach (PVA). The three-phase currents are projected in a fixed orthornormal reference frame with respect to the rotating field of the machine. This results in two quadrature currents $i_\alpha(t)$ and $i_\beta(t)$, which are sinusoidal and of the same frequency as the measured currents. The Concordia transform is defined by the following matrix relation:

$$i_{\alpha\beta o}(t) = \sqrt{\frac{2}{3}} \begin{bmatrix} 1 & -\frac{1}{2} & -\frac{1}{2} \\ 0 & \frac{\sqrt{3}}{2} & -\frac{\sqrt{3}}{2} \\ \frac{1}{\sqrt{2}} & \frac{1}{\sqrt{2}} & \frac{1}{\sqrt{2}} \end{bmatrix} \begin{bmatrix} i_a(t) \\ i_b(t) \\ i_c(t) \end{bmatrix} \tag{9}$$

This transformation allows us to define a rotating vector characterized by its instantaneous amplitude and phase, respectively $IA(t)$, $IP(t)$:

$$IA(t) = \sqrt{I_\alpha^2(t) + I_\beta^2(t)} \tag{10}$$

$$IP(t) = atan(\frac{I_\beta(t)}{I_\alpha(t)}) \tag{11}$$

We can also define the instantaneous pulsation and the frequency $IW(t)$ and $IF(t)$ respectively:

$$IF(t) = \frac{IW(t)}{2\pi} = \frac{1}{2\pi} \dot{IP}(t) \tag{12}$$

The main limitation of the Concordia transform is that the three-phase currents must be balanced. The first alternative is to use the Fortescu transform. It allows, from an unbalanced three-phase system, the generation of three balanced direct, inverse, and homo-polar systems. A second alternative is principal component analysis (PCA) [57].

In this paper, the motor has been considered to have a constant speed and run according to the operating characteristics mentioned in Table 2. On this basis, the signal processing technique used to analyze the current was the Fast Fourier Transform (FFT). The FFT served as a bridge between the temporal domain and the frequency domain, and it is the most widely used signal processing method when treating stationary signals [58]. In the event of a system malfunction, this results in the creation of certain frequencies (f_s) that appear in the analysis of the spectrum of IA or IF as shown in Equation (13), where each frequency represents a specific defect. Note that f_d is the defect frequency as indicated in Table 3, and $K = 1, 2, \ldots n$. In the next section, a statistical-based approach is used for defect detection.

$$f_s = K * f_d \tag{13}$$

After knowing the effect of the faults on the electric current, we move on to the next step, which is to determine the severity of each one.

2.4. Diagnostic Protocol: Statistical Method

To set up a diagnostic protocol, an alarm must be triggered automatically when a defect occurs. Then, a specific signature threshold must be defined. To accomplish this in a noisy situation, the statistical approach is a robust solution. A statistical diagnostic approach is proposed by [59,60] for the conditions of speed variation. This approach proposes two stages: a learning stage and a diagnostic stage. The chosen defect signature is the amplitude of the frequency corresponding to the defect in the rotational speed signal:

$$S_{defect} = \mid \hat{f}_m(f_d) \mid \tag{14}$$

In the learning phase, a statistical reference of the health status is generated. For this purpose, N_{ref} registrations are recorded. Then, the fault signature $S_{defect}(k)$ of each record is determined. The mean μ and standard deviation σ statistical characteristics are calculated as follows:

$$\hat{\mu}_{ref} = \frac{1}{N_{ref}} \sum_{k=1}^{N_{ref}} S_{defect}(k) \tag{15}$$

$$\hat{\sigma}_{ref} = \sqrt{\frac{1}{N_{ref} - 1} \sum_{k=1}^{N_{ref}} (S_{defect}(k) - \hat{\mu}_{ref})^2} \tag{16}$$

To make the signature independent of the machine type, a centered reduced signature is defined as shown in Equation (17)

$$S_{defect,RC}(k) = \frac{S_{defect}(k) - \hat{\mu}_{ref}}{\hat{\sigma}_{ref}} \tag{17}$$

A threshold could be defined to automatically trigger a defective state alarm. A probability of 1% is derived from the Gaussian distribution with Equations (18), while the probability is calculated as Equation (19)

$$P(S_{defect,RC}(k) > t_{1\%}) = 0,01 \tag{18}$$

$$P(S_{defect,RC}(k) > t) = 1 - \Phi(t), \tag{19}$$

The alarm threshold for a probability of 1% indicates that when the alarm is launched to declare a faulty state, there is a 1% chance that it is a false alarm. This probability can be modified according to the application used (0.1% for instance). The diagnostic phase can now begin after defining the threshold of the alarm.

This is a simple approach when the rotating speed is fixed. It becomes more complicated for variable-speed conditions. A solution is suggested by [60] based on dividing the speed–torque into N zones. A standardized reference and an alarm threshold are generated

for each zone in the learning phase. Then, when the diagnostic phase begins, the torque and speed of the unit are computed to allow the determination of a particular operating zone of the unit in the speed–torque plane. The decision is made based on this particular zone.

After completing the modeling and explaining the methodologies that will be used in this paper, the experimental and simulation results are presented and discussed in the next section.

3. Results and Discussions

First, the three-phases currents obtained from the physical and the Simulink model in the ideal condition, without any system defects, are collected. The data acquisition device utilized to collect currents from the physical fan/motor system, with its implementation presented in Figure 8. This tool has a filter up to 2.5 KHz. Note that all measurements were collected for 60 s when the current reached its steady state.

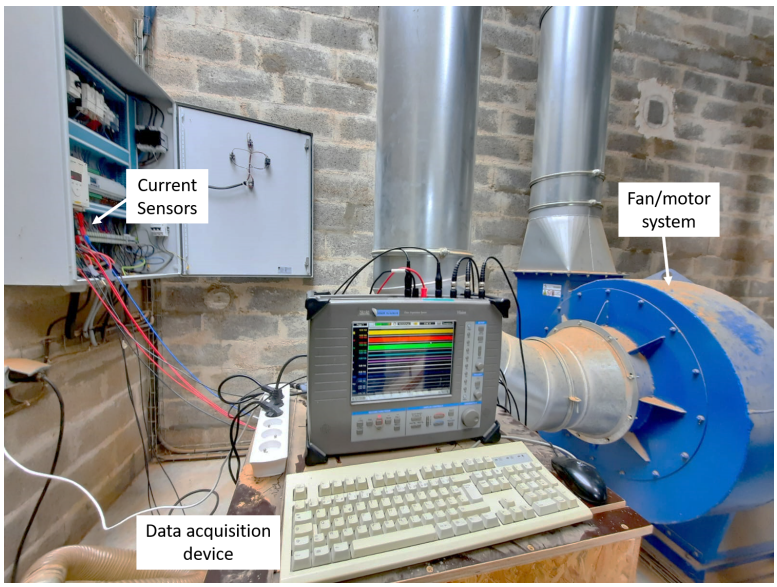

Figure 8. The data acquisition system.

One phase current of each case are shown in Figure 9. This image shows an almost perfect match between the two currents with a slight difference in amplitudes. The simulated current has a slightly higher value than the measured one. The RMS error between these currents is demonstrated is equal to 4641.

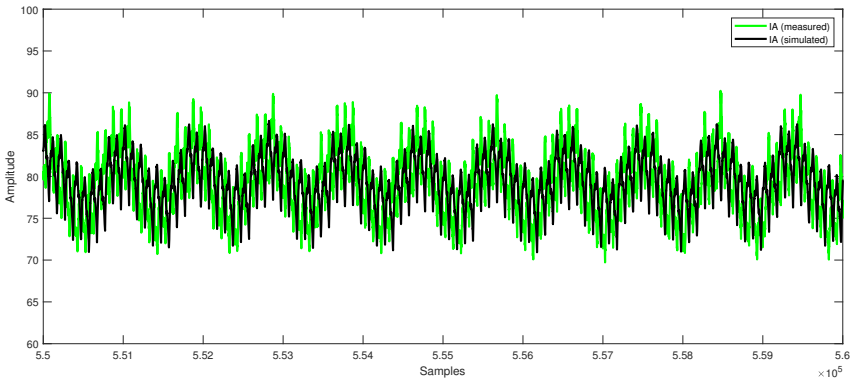

Figure 9. Simulated and measured one phase currents, from 55.5 to 56 s.

Then, and in order to dig deeper by analyzing these signals, we applied the concordia analysis, and we presented the results in Figures 10 and 11.

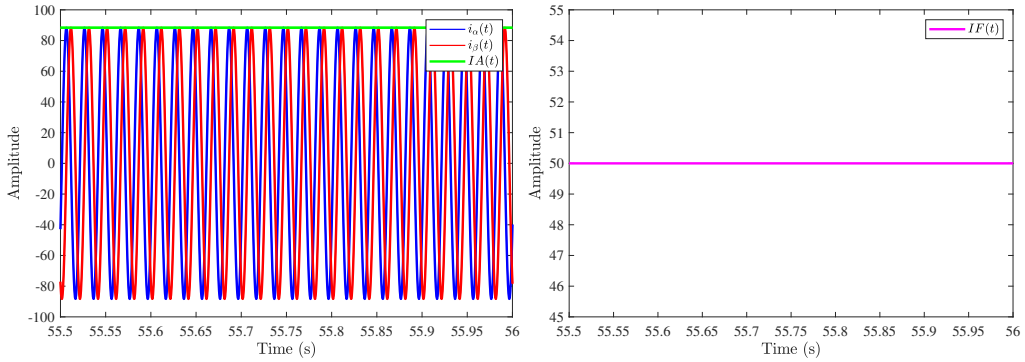

Figure 10. Simulated currents in the Concordia reference frame, from 55.5 to 56 s.

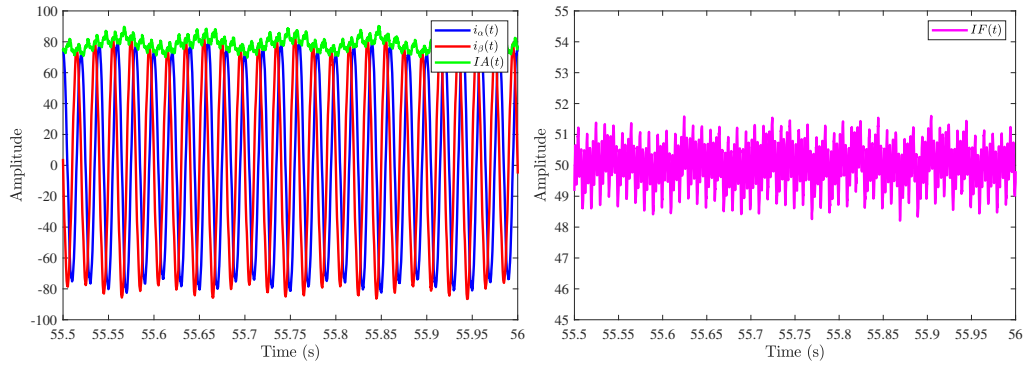

Figure 11. Measured currents in the Concordia reference frame, from 55.5 to 56 s.

Figures 10 demonstrates that both currents IA and IF appear to be without any disturbance, and this is the normal state, because the modeled system is an ideal system free of defects, so the current is exempt from any frequency other than the main frequency of the 50 Hz value. As for Figure 11, it is not the same, and the disturbances affect these currents. Knowing that the signal taken from the actual system was picked when the system operates in normal conditions without any defects, the RMS error between the meaured and the simulated IA is equal to 10.1551. What we can conclude from this figure is that the current contains other frequencies, unlike the simulated current, and these frequencies do not necessarily mean that there are malfunctions in the system. Thus, we decided to take this current and analyze it using the FFT analysis. Figure 12 shows the FFT for $IA(t)$ and $IF(t)$ in the case of measured currents.

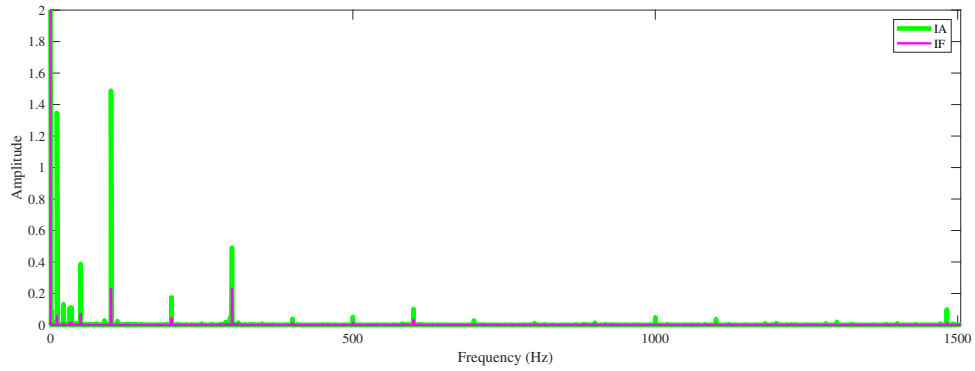

Figure 12. FFT of IA and IF for the measured currents.

The spectrum analysis showed that the source of the disturbances affecting the modulated current is the appearance of frequencies that were not found in the ideal case from the Simulink model. When looking more carefully at the value of these frequencies, it can

be seen that a specter appeared at 1.39 Hz, which, according to Table 3, represents the rotor rod, while the one which appeared at 10.68 Hz represents the belts' frequency. The specter at 50 Hz represents the electrical supply frequency. In addition to these frequencies, the FFT shows a set of frequencies that initially appeared at 100 Hz and then repeated according to Equation (13), which indicates the existence of a level of misalignment, while the small specter at 1450 represents the harmonics resulting from the stator notches, as indicated in Table 3.

The appearance of these disturbances does not necessarily mean that the system is no longer functioning or that the component causing this frequency must be replaced. The fan/motor system of the MTC on which the measurements were made was working well. Therefore, to make the Simulink model as close to reality as possible, these frequencies were then added to it through the parameter T_d obtained from Equation (5) and inserted into Equation (4). Thus, the spectral analysis of the simulated IA becomes as shown in Figure 13, which also shows the FFT of that obtained from the measured currents in order to be able to compare them. It should be noted that the instantaneous amplitude was used, as the frequencies are more apparent there than in IF, as demonstrated by Figure 12. The other frequencies presented in the measured IA result from fault harmonics and noise in the current. Due to their small amplitude relative to the other components, they are not simulated in the model.

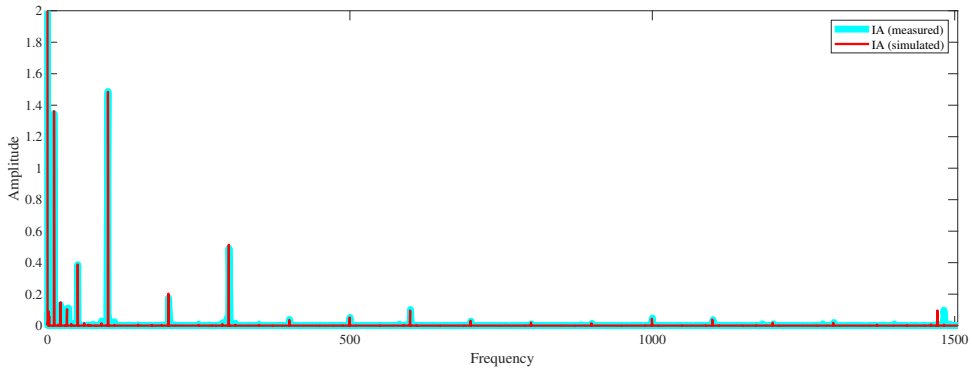

Figure 13. FFT of the measured and simulated IA.

Figure 14 shows how the simulated IA became after making the changes to the digital twin. Some disturbances affected it that were not present in the ideal condition (Figure 10). Additionally, Figure 14 demonstrates a comparison with the measured IA and shows that the simulated one becomes close to reality. The RMS error between these two currents is decreased from 10.1551 in to 5.232. Therefore, since these disturbances or all these frequencies do not mean the presence of a malfunction, as we have mentioned, it is necessary to develop a diagnostic approach that can trigger an alarm when faults appear and reach a certain margin level. In this part, we test the procedure described in the previous section. For that, the simulator of the motor/fan system of the MTC already detailed in Section 2.1 is used.

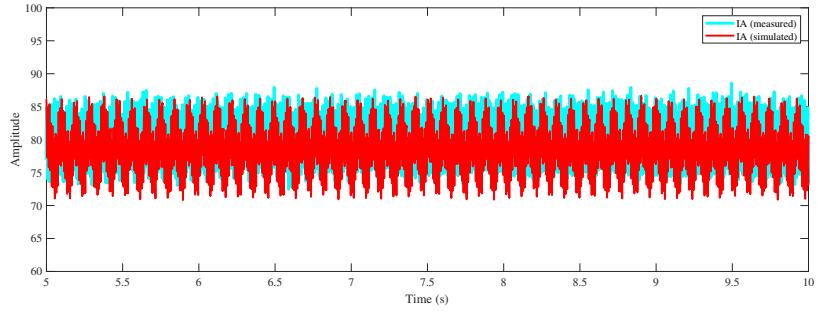

Figure 14. Simulated and measured $IA(t)$, from 5 to 6 s.

In this simulation, the test is performed on 30 recordings in a healthy operating state at a fixed speed and steady state. Each recording is for a recording time of about 2 min. In order to facilitate the simulation, we limit ourselves to only one type of fault. We will consider in this part that the concerned fault is that of the transmission belt, because it has the highest magnitude, as shown in Figures 12 and 13. For a complete simulation of the monitoring by statistical analysis, the same approach can be done for the rest of the possible defects defined in Table 3, by using Equation (17) to create a centered, reduced signature that can be applied to all defect types. In particular, for the rotor bar defect there is an approach that has been formulated by [57] based on many experiments and readings to determine its severity, through which the margin level of the frequency magnitude can be determined.

The recordings without defects were made on the real motor/fan system on the MTC site at a fixed speed (Figure 8). With the impossibility of creating a fault in the existing system, the recordings with fault were estimated by the simulation of the digital twin presented in Section 2.2, by creating a fault on the transmission belts while taking into account white noise, in order to reach as close as possible to reality.

In the training stage, $N_{ref} = 30$ registrations are gathered from the physical system. Each registration represents a single measurement with a duration of 60 s. The fault signatures S_{defect} are computed. The normalized reference is then generated. The threshold for a 1% probability is calculated as 2.33. Then, a belt fault was generated using the Simulink model, only because, in the real situation, we can not create a fault in the industrial system. Then, this fault is compared with the threshold. Figure 15 shows the distribution of the normalized signatures, while the comparison of the healthy and faulty condition of the system compared to the threshold is shown in Figure 16.

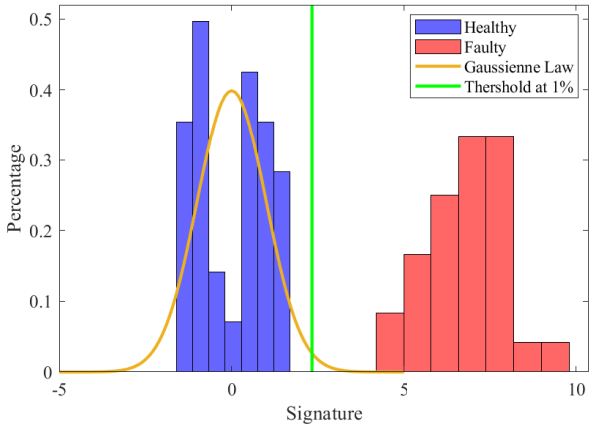

Figure 15. Histogram distribution of fault signatures using 30 measures.

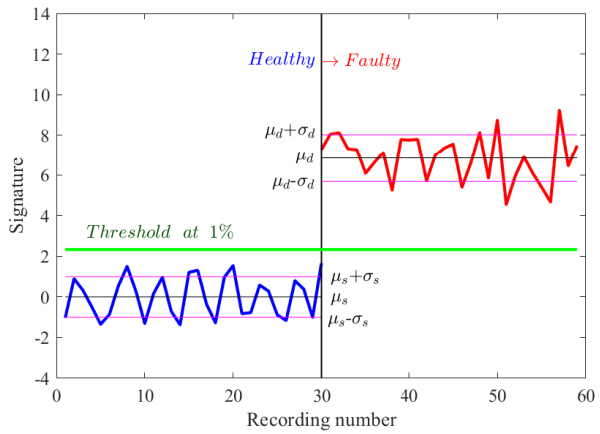

Figure 16. Fault signatures using 30 measures.

4. Conclusions

This article discusses the topic of condition monitoring in ventilation systems based on the digital twin approach. The most common defects in this type of system have been reviewed. The method adopted in the diagnostic process is the MCSA, where the Concordia method and the FFT analysis are used to process the current signal. An alarm has been created to determine the severity of the defects. We now have a reference that allows for the state that the real system should be in. Experimental and simulation results prove the effectiveness of this developed technique. The use of this approach has been limited to ventilation systems, but with some modifications, it can be used with different frameworks.

Finally, as a proposal of future works, the developed approach can be used with other types of industrial systems and different kinds of defects. Other techniques can also be adopted in processing the current signals. Another topic of research is the implementation of the artificial intelligence, such as Artificial Neural Networks and Fuzzy and Neuro-Fuzzy logic, to create the alarm that determines the severity of the defects instead of a statistical study. This study deals with a system that operates at fixed speeds. In order to improve the efficiency of the system to handle different operating environments, it is possible to implement signal processing algorithms (such as adaptive notch filters and adaptive observer approach) that can track and estimate transient frequencies to detect faults in variable speed conditions.

Author Contributions: S.C., E.E. and L.R. proposed the main idea of the paper; M.F.Y. developed the digital twin. M.F.Y. and H.H. took measurements from the MTC. M.F.Y., H.H. and S.C. implemented simulation verification, analyses, and experimental tests. M.F.Y. and A.S. developed the statistical approach. The paper was written by M.F.Y., H.H. and S.C., and was revised by E.E., L.R. and A.S. All the authors were involved in preparing the final version of this manuscript. Besides, this whole work is supervised by S.C., A.S., H.A. and M.E.-G. All authors have read and agreed to the published version of the manuscript.

Funding: This research was funded by the French Embassy in Lebanon and Beirut Arab University.

Institutional Review Board Statement: Not applicable.

Data Availability Statement: Data are available upon request from the corresponding author.

Acknowledgments: The authors would like to thank everyone who contributed to the realization of this research, either academically or through financial support. The authors are grateful to the Municipal Technical Center of Poitiers for providing the necessary data and access to the company's equipment.

Conflicts of Interest: The authors declare no conflict of interest.

Abbreviations

The following abbreviations are used in this manuscript:

CM	Condition monitoring
IM	Induction motor
MCSA	Motor current signature analysis
MTC	Municipal technical centre

Appendix A

1 Turbine
2 Seat
3 Scroll
4 Entrance pavilion
5 Motor with sliders
6 Shaft connection
7 Transmission

8	Shaft casing and baring
9	Transmission casing
10	Frame
11	Reinforced sealing system (option)
12	Rotation detector (option)
a	Pulley 1
b	Pulley 2
c	Belts
d	Bearings
e	Shaft
f	Fan

References

1. Mattera, C.G.; Quevedo, J.; Escobet, T.; Shaker, H.R.; Jradi, M. A Method for Fault Detection and Diagnostics in Ventilation Units Using Virtual Sensors. *Sensors* **2018**, *18*, 3931. [CrossRef]
2. Kaya, D.; Çanka Kılıç, F.; Öztürk, H.H. *Energy Management and Energy Efficiency in Industry: Practical Examples*; Chapter Energy Efficiency in Fans; Springer International Publishing: Cham, Switzerland, 2021; pp. 419–425. [CrossRef]
3. Diab, A.A.Z.; Al-Sayed, A.H.M.; Mohammed, H.H.A.; Mohammed, Y.S. *Development of Adaptive Speed Observers for Induction Machine System Stabilization*; Chapter Literature Review of Induction Motor Drives; Springer: Singapore, 2020; pp. 7–18. [CrossRef]
4. Jin, X.; Chow, T.W. Anomaly detection of cooling fan and fault classification of induction motor using Mahalanobis–Taguchi system. *Expert Syst. Appl.* **2013**, *40*, 5787–5795. [CrossRef]
5. Kang, T.J.; Yang, C.; Park, Y.; Hyun, D.; Lee, S.B.; Teska, M. Electrical Monitoring of Mechanical Defects in Induction Motor-Driven V-Belt–Pulley Speed Reduction Couplings. *IEEE Trans. Ind. Appl.* **2018**, *54*, 2255–2264. [CrossRef]
6. Yan, X.; Jia, M.; Zhang, W.; Zhu, L. Fault diagnosis of rolling element bearing using a new optimal scale morphology analysis method. *ISA Trans.* **2018**, *73*, 165–180. [CrossRef]
7. Glowacz, A.; Glowacz, W.; Glowacz, Z.; Kozi, J. Early fault diagnosis of bearing and stator faults of the single-phase induction motor using acoustic signals. *Measurement* **2018**, *113*, 1–9. [CrossRef]
8. Bazan, G.H.; Scalassara, P.R.; Endo, W.; Goedtel, A.; Godoy, W.F.; Palácios, R.H.C. Stator fault analysis of three-phase induction motors using information measures and artificial neural networks. *Electr. Power Syst. Res.* **2017**, *143*, 347–356. [CrossRef]
9. Gonzalez-Cordoba, J.L.; Osornio-Rios, R.A.; Granados-Lieberman, D.; Romero-Troncoso, R.d.J.; Valtierra-Rodriguez, M. Thermal-Impact-Based Protection of Induction Motors Under Voltage Unbalance Conditions. *IEEE Trans. Energy Convers.* **2018**, *33*, 1748–1756. [CrossRef]
10. Sahu, S.; Dash, R.N.; Panigrahi, C.K.; Subudhi, B. Unbalanced voltage effects and its analysis on an induction motor. In Proceedings of the International Conference on Innovative Mechanisms for Industry Applications (ICIMIA), Bengaluru, India, 21–23 February 2017; pp. 263–268. [CrossRef]
11. Panagiotou, P.A.; Arvanitakis, I.; Lophitis, N.; Antonino-Daviu, J.A.; Gyftakis, K.N. A New Approach for Broken Rotor Bar Detection in Induction Motors Using Frequency Extraction in Stray Flux Signals. *IEEE Trans. Ind. Appl.* **2019**, *55*, 3501–3511. [CrossRef]
12. Asad, B.; Vaimann, T.; Belahcen, A.; Kallaste, A.; Rassolkin, A.; Heidari, H. The Low Voltage Start-up Test of Induction Motor for the Detection of Broken Bars. In Proceedings of the International Conference on Electrical Machines (ICEM), Online, 23–26 August 202; pp. 1481–1487. [CrossRef]
13. Oumaamar, M.E.K.; Maouche, Y.; Boucherma, M.; Khezzar, A. Static air-gap eccentricity fault diagnosis using rotor slot harmonics in line neutral voltage of three-phase squirrel cage induction motor. *Mech. Syst. Signal Process.* **2017**, *84*, 584–597. [CrossRef]
14. Yassa, N.; Rachek, M.; Houassine, H. Motor Current Signature Analysis for the Air Gap Eccentricity Detection In the Squirrel Cage Induction Machines. *Energy Procedia* **2019**, *162*, 251–262. [CrossRef]
15. Jokic, S.; Cincar, N.; Novakovic, B. The analysis of vibration measurement and current signature in motor drive faults detection. In Proceedings of the 17th International Symposium INFOTEH-JAHORINA (INFOTEH), Sarajevo, Bosnia and Herzegovina, 21–23 March 2018; pp. 1–6. [CrossRef]
16. Gangsar, P.; Tiwari, R. Signal based condition monitoring techniques for fault detection and diagnosis of induction motors: A state-of-the-art review. *Mech. Syst. Signal Process.* **2020**, *144*, 106908. [CrossRef]
17. Han, Q.; Ding, Z.; Xu, X.; Wang, T.; Chu, F. Stator current model for detecting rolling bearing faults in induction motors using magnetic equivalent circuits. *Mech. Syst. Signal Process.* **2019**, *131*, 554–575. [CrossRef]
18. Toma, R.N.; Prosvirin, A.E.; Kim, J.M. Bearing Fault Diagnosis of Induction Motors Using a Genetic Algorithm and Machine Learning Classifiers. *Sensors* **2020**, *20*, 1884. [CrossRef]
19. Hossain, M.L.; Abu-Siada, A.; Muyeen, S.M. Methods for Advanced Wind Turbine Condition Monitoring and Early Diagnosis: A Literature Review. *Energies* **2018**, *11*, 1309–1322. [CrossRef]
20. Arun, A.; Rameshkumar, K.; Unnikrishnan, D.; Sumesh, A. Tool Condition Monitoring Of Cylindrical Grinding Process Using Acoustic Emission Sensor. *Mater. Today Proc.* **2018**, *5*, 11888–11899. [CrossRef]

21. Choudhary, A.; Goyal, D.; Shimi, S.L.; Akula, A. Condition Monitoring and Fault Diagnosis of Induction Motors: A Review. *Arch. Comput. Methods Eng.* **2019**, *26*, 1221–1238. [CrossRef]
22. Schoen, R.; Habetler, T. Effects of time-varying loads on rotor fault detection in induction machines. In Proceedings of the 1993 IEEE Industry Applications Conference TwentyEighth IAS Annual Meeting, Toronto, ON, Canada, 2–8 October 1993; pp. 324–330. [CrossRef]
23. Saad, N.; Irfan, M.; Ibrahim, R. *Condition Monitoring and Faults Diagnosis of Induction Motors: Electrical Signature Analysis*; CRC Press: Boca Raton, FL, USA, 2018.
24. Thomson, W.T.; Culbert, I. Current signature analysis for condition monitoring of cage induction motors: Industrial application and case Histories, first edition. In Proceedings of the International Conference on Electrical, Electronics, and Optimization Techniques (ICEEOT 2016), Chennai, India, 3–5 March 2016.
25. Boschert, S.; Rosen, R. *Digital Twin—The Simulation Aspect*; Springer: Berlin/Heidelberg, Germany, 2016.
26. Grieves, M. Manufacturing Excellence through Virtual Factory Replication. *White Pap.* **2015**, *1*, 1–7.
27. Negri, E.; Fumagalli, L.; Macchi, M. A review of the roles of digital twin in CPS-based production system. *Procedia Manuf.* **2017**, *11*, 939–948. [CrossRef]
28. Tuegel, E.J.; Ingraffea, A.R.; Eason, T.G.; Spottswood, S.M. Reengineering aircraft structural life prediction using a digital twin. *Int. J. Aerosp. Eng.* **2011**, *2011*, 154798. [CrossRef]
29. Abramovici, M.; Göbel, J.C.; BaoDang, H. Semantic data management for the development and continuous reconfiguration of smart products and systems. *CIRP Annals* **2016**, *65*, 185–188. [CrossRef]
30. Rosen, R.; Wichert, G.; Lo, G.; Bettenhausen, K.D. About the importance of autonomy and digital twins for the future of manufacturing. *CIRP Annals* **2015**, *48*, 567–572. [CrossRef]
31. Schluse, M.; Rossmann, J. From simulation to experimentable digital twins: Simulation-based development and operation of complex technical systems. In Proceedings of the IEEE International Symposium on Systems Engineering (ISSE), Edinburgh, UK, 3–5 October 2016; pp. 1–6. [CrossRef]
32. Kraft, E.M. The Air Force Digital Thread/Digital Twin—Life Cycle Integration and Use of Computational and Experimental Knowledge. In Proceedings of the 54th AIAA Aerospace Sciences Meeting, AIAA SciTech Forum (AIAA 2016-0897), Grapevine, TX, USA, 9–13 January 2017; pp. 1–22. [CrossRef]
33. Aivaliotis, P.; Georgoulias, K.; Alexopoulos, K. Using digital twin for maintenance applications in manufacturing: State of the Art and Gap analysis. In Proceedings of the IEEE International Conference on Engineering, Technology and Innovation (ICE/ITMC), Park, France, 17–19 June 2019; pp. 1–5. [CrossRef]
34. Chowdhury, S.; Yedavalli, R.K. Dynamics of belt-pulley-shaft systems. *Mech. Mach. Theory* **2016**, *98*, 199–215. [CrossRef]
35. Fu, C.; Xu, Y.; Yang, Y.; Lu, K.; Gu, F.; Ball, A. Response analysis of an accelerating unbalanced rotating system with both random and interval variables. *J. Sound Vib.* **2020**, *466*, 115047. [CrossRef]
36. Yu, P.; Zhang, D.; Ma, Y.; Hong, J. Dynamic modeling and vibration characteristics analysis of the aero-engine dual-rotor system with Fan blade out. *Mech. Syst. Signal Process.* **2018**, *106*, 158–175. [CrossRef]
37. Yakhni, M.F.; Ali, M.N.; El-Goary, M.A. Magnetorheological damper voltage control using artificial neural network for optimum vehicle ride comfort. *J. Mech. Eng. Sci.* **2021**, *15*, 7648–7661. [CrossRef]
38. Luo, W.; Hu, T.; Zhang, C.; Wei, Y. Digital twin for CNC machine tool: Modeling and using strategy. *J. Ambient. Intell. Humaniz. Comput.* **2019**, *10*, 1129–1140. [CrossRef]
39. Afrizal, N. Motor Current Signature Analysis towards Mechanical Seal Failure Detection for Electrical Submersible Pump. Ph.D. Thesis, University of Liverpool, Liverpool, UK, 2020.
40. Xia, M.; Shao, H.; Williams, D.; Lu, S.; Shu, L.; de Silva, C.W. Intelligent fault diagnosis of machinery using digital twin-assisted deep transfer learning *Reliab. Eng. Syst. Saf.* **2021**, *215*, 107938. [CrossRef]
41. Xiao, Y.; Shao, H.; Han, S.; Huo, Z.; Wan, J. Novel Joint Transfer Network for Unsupervised Bearing Fault Diagnosis From Simulation Domain to Experimental Domain. *IEEE/ASME Trans. Mechatron.* **2022**, *215*, 1–10. [CrossRef]
42. Wang, J.; Ye, L.; Gao, R.X.; Li, C.; Zhang, L. Digital Twin for rotating machinery fault diagnosis in smart manufacturing. *Int. J. Prod. Res.* **2019**, *57*, 3920–3934. [CrossRef]
43. Noureddine, B.; Eddine, Z.S.; Mohamed, S. Experimental exploitation for the diagnosis to the induction machine under a bearing fault—Using MCSA. In Proceedings of the 4th International Conference on Electrical Engineering (ICEE), Boumerdes, Algeria, 13–15 December; pp. 1–4. [CrossRef]
44. Hyun, D.; Kang, T.J.; Kim, J. Fault diagnosis of belt driving power transfer facility using vibration analysis. *J. Electr. Eng. Technol.* **2021**, *16*, 2257–2264. [CrossRef]
45. Singh, G.; Naikan, V. Detection of half broken rotor bar fault in VFD driven induction motor drive using motor square current MUSIC analysis. *Mech. Syst. Signal Process.* **2018**, *110*, 333–348. [CrossRef]
46. Thomson, W.T.; Culbert, I. *Current Signature Analysis for Condition Monitoring of Cage Induction Motors: Industrial Application and Case Histories;* John Wiley & Sons: Hoboken, NJ, USA, 2017.
47. Dehina, W.; Boumerhaz, M.; Kraftz, F.; Fantini, J. Diagnosis and Comparison between Stator Current Analysis and Vibration Analysis of Static Eccentricity Faults in The Induction Motor. In Proceedings of the 4th International Conference on Power Electronics and their Applications (ICPEA), Elazig, Turkey, 25–27 September 2019; pp. 1–4. [CrossRef]

48. Fournier, E.; Picot, A.; Régnier, J.; Andrieux, C.; Saint-Michel, J.; Maussion, P. Effects of transmission belt looseness on electrical and mechanical measurements of an induction motor. In Proceedings of the 2015 IEEE 10th International Symposium on Diagnostics for Electrical Machines, Power Electronics and Drives (SDEMPED), Guarda, Portugal, 1–4 September 2015; pp. 259–265. [CrossRef]
49. Marzebali, M.H.; Kia, S.H.; Henao, H.; Capolino, G.A.; Faiz, J. Planetary Gearbox Torsional Vibration Effects on Wound-Rotor Induction Generator Electrical Signatures. *IEEE Trans. Ind. Appl.* **2016**, *52*, 4770–4780. [CrossRef]
50. Allouche, A.; Etien, E.; Rambault, L.; Doget, T.; Cauet, S.; Sakout, A. Mechanical Fault Diagnostic in PMSM from Only One Current Measurement: A Tacholess Order Tracking Approach. *Sensors* **2020**, *20*, 5011. [CrossRef]
51. Elvira-Ortiz, D.A.; Morinigo-Sotelo, D.; Zorita-Lamadrid, A.L.; Osornio-Rios, R.A.; Romero-Troncoso, R.D.J. Fundamental frequency suppression for the detection of broken bar in induction motors at low slip and frequency. *Appl. Sci.* **2020**, *10*, 4160. [CrossRef]
52. Etien, E.; Allouche, A.; Rambault, L.; Doget, T.; Cauet, S.; Sakout, A. A Tacholess Order Analysis Method for PMSG Mechanical Fault Detection with Varying Speeds. *Electronics* **2021**, *10*, 418. [CrossRef]
53. Li, H.; Wang, Z.; Zhen, D.; Gu, F.; Ball, A. Modulation Sideband Separation Using the Teager–Kaiser Energy Operator for Rotor Fault Diagnostics of Induction Motors. *Energies* **2019**, *12*, 4437. [CrossRef]
54. Trajin, B.; Chabert, M.; Regnier, J.; Faucher, J. Hilbert versus Concordia transform for three-phase machine stator current time-frequency monitoring. *Mech. Syst. Signal Process.* **2009**, *23*, 2648–2657. [CrossRef]
55. Elbouchikhi, E.; Choqueuse, V.; Amirat, Y.; Benbouzid, M.E.H.; Turri, S. An Efficient Hilbert–Huang Transform-Based Bearing Faults Detection in Induction Machines. *IEEE Trans. Energy Convers.* **2017**, *32*, 401–413. [CrossRef]
56. Choqueuse, V.; Benbouzid, M.E.H.; Amirat, Y.; Turri, S. Diagnosis of Three-Phase Electrical Machines Using Multidimensional Demodulation Techniques. *IEEE Trans. Ind. Electron.* **2012**, *59*, 2014–2023. [CrossRef]
57. Bouchikhi, E.H.E.; Choqueuse, V.; Benbouzid, M.; Antonino-Daviu, J.A. Stator current demodulation for induction machine rotor faults diagnosis. In Proceedings of the First International Conference on Green Energy ICGE 2014, Sfax, Tunisia, 25–27 March 2014; pp. 176–181. [CrossRef]
58. Pin, G.; Wang, Y.; Chen, B.; Parisini, T. Identification of multi-sinusoidal signals with direct frequency estimation: An adaptive observer approach. *Automatica* **2019**, *99*, 338–345. [CrossRef]
59. Fournier, E.; Picot, A.; Regnier, J.; Maussion, P.; Yamdeu, M.T.; Andrejak, J.M.; Somer, L. A generic diagnosis protocol for the monitoring of induction motors based on multiple statistical references in the torque-speed plane. In Proceedings of the IECON 2014—40th Annual Conference of the IEEE Industrial Electronics Society, Dallas, TX, USA, 29 October–1 November 2014; pp. 3348–3354. [CrossRef]
60. Fournier, E.; Picot, A.; Régnier, J.; Yamdeu, M.T.; Andréjak, J.M.; Maussion, P. Current-Based Detection of Mechanical Unbalance in an Induction Machine Using Spectral Kurtosis With Reference. *IEEE Trans. Ind. Electron.* **2015**, *62*, 1879–1887. [CrossRef]